Supporting Information - The impact of chemical structure and molecular packing on the electronic polarisation of fullerene arrays [†]

Sheridan Few, Cleaven Chia, Daniel Teo, James Kirkpatrick, and Jenny Nelson

1   Construction of a Subcrystal

In constructing a subcrystal, it is first necessary to construct a unit cell. Atomic co-ordinates of each molecule in the unit cell are obtained using the Mercury software package,[3] following which, unit cells are defined in a different manner when using the atomic, and molecular, point dipole models.

In building a unit cell using the molecular point dipole model, there is a challenge of rotating the calculated polarisability tensor for a molecule in an optimised geometry, $\boldsymbol{\alpha}_{QC}$ to polarisability tensors corresponding to molecules orientated as in the unit cell, $\boldsymbol{\alpha}_{cif}$. This is achieved in the following manner: First, atomic co-ordinates of the geometry-optimised molecule are extracted, and displaced such that the molecule's centre of mass (or centre of the cage for fullerene molecules) lies at (0,0,0). Second, the atomic co-ordinates of a molecule in the unit cell in the desired orientation are extracted, and these co-ordinates are displaced in a similar manner. Third, two atoms are selected with which to align the molecules. The first of these atoms (atom 'a' in Figure 1) is chosen at an extremity of the molecule, and the second of these atoms (atom 'b' in Figure 1) as far as possible from the vector joining the centre of the molecule to atom 'a'. Both atoms are rigidly connected to the molecules core (as opposed to attached to a flexible alkyl sidechain). An example for PCBM is shown in Figure 1.

Fourth, a rotation matrix $\boldsymbol{R}_a$ is defined to align atom 'a' in the two geometries, and the optimised co-ordinates rotated. Vectors $\vec{v}_{a,QC}$, and $\vec{v}_{a,cif}$ (with corresponding unit vectors $\hat{\vec{v}}_{a,QC}$ and $\hat{\vec{v}}_{a,cif}$) are defined, which join the point (0,0,0) to atom 'a' in the optimised, and .cif molecular geometries, respectively. A third unit vector, $\hat{\vec{v}}_{perp,a}$, is defined, perpendicular to the first two, by:
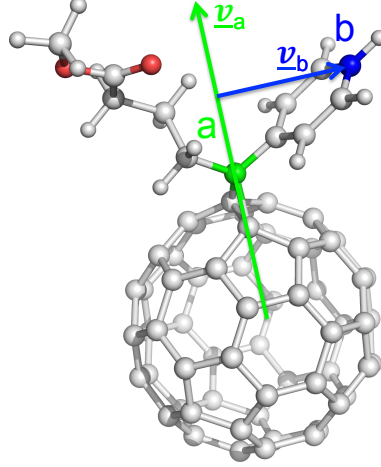
Figure 1 Atoms and Vectors for Polarisability Tensor Rotation in PCBM.

$$\vec{\hat{v}}_{perp,a} = \frac{\vec{\hat{v}}_{a,QC} \times \vec{\hat{v}}_{a,cif}}{|\vec{\hat{v}}_{a,QC} \times \vec{\hat{v}}_{a,cif}|} \tag{1}$$

The angle between vectors $\vec{\hat{v}}_{a,QC}$ and $\vec{\hat{v}}_{a,cif}$ is obtained by $\theta_a = arccos(\vec{\hat{v}}_{a,QC} \cdot \vec{\hat{v}}_{a,cif})$, and a rotation matrix, $\boldsymbol{R}_a$, is defined using Rodrigues formula[4] to rotates by θ_a about $\vec{\hat{v}}_{perp,a}$. This rotation matrix is applied to co-ordinates of the optimised geometry, aligning atom 'a' in the optimised geometry with atom 'a' in the .cif geometry.

Fifth, a second rotation matrix, $\boldsymbol{R}_b$, is defined to bring the two molecules into a similar orientation. A second pair of vectors, $\vec{v}_{b,QC}$, $\vec{v}_{b,cif}$ are defined, which represent the shortest vector joining a line in the direction of $\vec{\hat{v}}_{a,cif}$ to atom 'b' in the rotated optimised, and .cif geometries, respectively. A similar procedure to the above is applied to obtain the second rotation matrix, $\boldsymbol{R}_b$, which effects a rotation in the rotated optimised geometry, such that atom 'b' aligns with atom 'b' in the .cif geometry. Finally, these rotation matrices are successively applied to $\boldsymbol{\alpha_{QC}}$ to obtain a rotated polarisability tensor, $\boldsymbol{\alpha_{cif}} = \boldsymbol{R}_b\boldsymbol{R}_a\boldsymbol{\alpha_{QC}}$.

Following rotation of the polarisability tensor, a molecular point dipole with polarisability tensor $\boldsymbol{\alpha}_{cif}$ corresponding to the orientation of the particular molecule in the unit cell is placed at the centre of mass of the fullerene cage in the .cif file. This procedure is repeated for each molecule in the unit cell.

Having constructed a unit cell, a lattice is built up by replicating this unit cell, and translating these replicas according to translation vectors obtained from crystal parameters in .cif files. Lattices are built

either up to a specified maximum total number of translation vectors from the centre, or up to a maximum number of translation vectors in each direction, as indicated in discussion of results.

2   Calculation of Effective Dielectric Constant

We introduce a method for the calculation of a dielectric constant associated with separation of charges in a lattice of polarisable molecules. As defined in Section 2.2 of the main text, this section uses quantities U_{qq}, U_{qd} and U_{dd} to refer to energies associated with charge-charge, charge-dipole, and dipole-dipole interactions, and $\boldsymbol{E}_{ext}$ and $\boldsymbol{\mu}$ refer to column vectors describing the electric field and dipole moment at each polarisable point.

Consider a lattice containing two charges, $+e$ and $-e$, separated by a distance r along a lattice vector. By the superposition principle, the column vector $\boldsymbol{E}_{ext}$ (defined in Equation 10 of the main text) in a lattice containing two charges is equal to the sum of $\boldsymbol{E}_{ext}$ vectors for the same lattice containing each charge alone. We will denote these vectors $\boldsymbol{E}_{tot}$, $\boldsymbol{E}_+$ and $\boldsymbol{E}_-$, respectively:

$$\boldsymbol{E}_{tot} = \boldsymbol{E}_+ + \boldsymbol{E}_- \tag{2}$$

By Equation 8 of the main text, this implies:

$$\boldsymbol{\mu}_{tot} = \boldsymbol{\mu}_+ + \boldsymbol{\mu}_- \tag{3}$$

Where $\boldsymbol{\mu}_{tot}$, $\boldsymbol{\mu}_+$, and $\boldsymbol{\mu}_-$ are the set of dipoles for the same system. Thus, the energy of the system containing two charges, U_{tot} is the result of the interaction of each charge with its polarisable surroundings, $U_p = U_+ + U_-$, and an additional stabilising contribution resulting from the interaction between the two charges, U_B, the screened Coulomb binding energy of the charge pair. Note that U_p here should be thought of as a comparative value between a lattice with different arrangements of charge, and not as an absolute value. In practice, quadrupole moments are likely to make a significant contribution to absolute values of polaron binding energies, not included in this model.
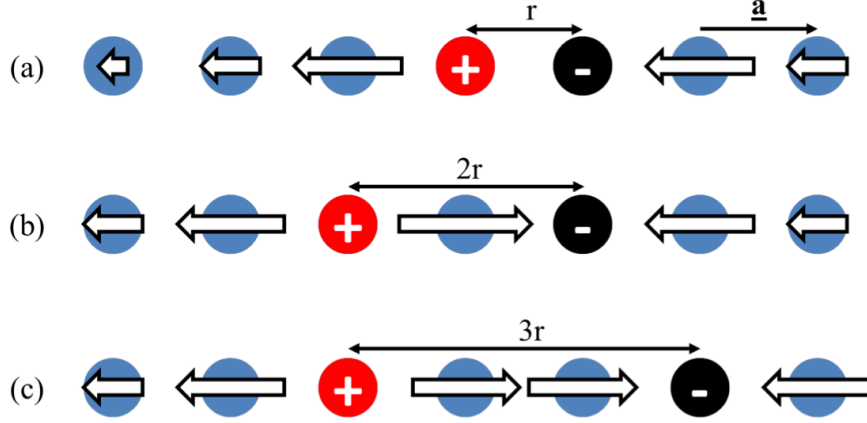
Figure 2 Calculation of Dielectric Tensor from the Point Dipole Model Schematic illustrating the varying of charge separation, from (a) r to (b) 2r and (c) 3r along the lattice vector a, in a lattice of polarisable points (blue circles) with dipole moments (white arrows, arrow length corresponds to dipole magnitude). Charges are separated by moving each charge from its current position to the corresponding point in the adjacent unit cell. This process is repeated until both charges are on polarisable points on the boundary of the lattice.

In this model, since $U_{qq} = 0$ for lattices containing only a single charge, this equation can be further simplified to $U_B = U_{qq} - \frac{1}{2}\left(\boldsymbol{\mu}_+ \cdot \boldsymbol{E}_- + \boldsymbol{\mu}_- \cdot \boldsymbol{E}_+\right)$.

$$U_B = U_{tot} - U_p \tag{4}$$

For charges separated by a distance r along a given axis, x it is possible to calculate an "effective dielectric constant", $\epsilon_{r,x}$, associated with charge separation along that axis, by applying a linear fit to the dependence of U_B upon separation of charges:

$$\epsilon_{r,x} = -\frac{d^1/\vec{r}_x}{dU_B} \tag{5}$$

Equation 5 is used to calculate effective dielectric constants associated with separation of a charge along different lattice vectors in a series of molecular systems as a function of lattice size and charge separation. Molecules of charge $+e$ and $-e$ are placed on equivalent sites in adjacent unit cells close to the centre of the lattice, separated by the lattice vector of interest (Figure 2). Charges are then separated along the lattice vector of interest until they reach the extremities of the subcrystal. A value of $\epsilon_{r,x}$ is extracted from the slope of U_B with inverse separation $\frac{1}{r}$ using Equation 5, at large values of $\frac{1}{r}$.

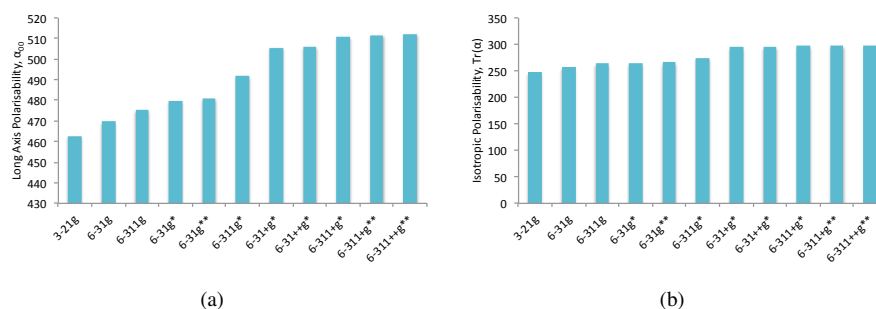(a)   (b)

Figure 3 Effect of Basis Set On Polarisability (a) long axis, and (b) isotropic polarisability of tetrathiophene as calculated using HF method with a range of basis sets.

3   Effect of Basis Set On Calculated Polarisability of Tetrathiophene

We calculate the polarisability of tetrathiophene using HF method with a range of Pople basis set sizes. The long-axis, and isotropic polarisabilities are shown in Figure 3.

Changes in long-axis polarisability with basis set size are proportionally larger than those in isotropic polarisability. Increasing basis set size from 6-31+g* to 6-311++g** results an increase of just over 1% in long-axis polarisability.

4   Quantum Chemical Polarisabilities

Anisotropies associated with the polarisability tensors of linear and cyclic molecules describes in the main text are presented in Figure 4. Calculated polarisability tensors are included in the accompanying excel spreadsheet.
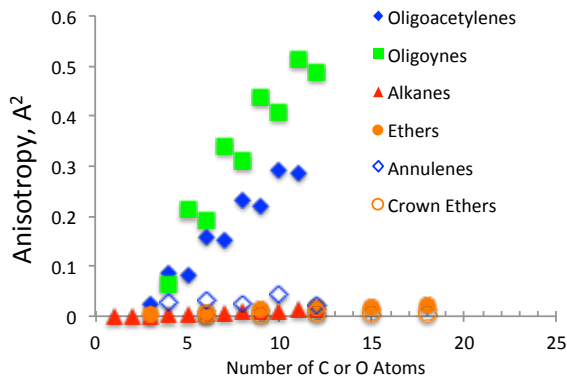
Figure 4 Anisotropy of Polarisabilities of Linear and Cyclic Molecules Anisotropy of polarisability tensors, as defined in the main text, for linear conjugated oligacetylenes and oligoynes, linear non-conjugated alkanes and oligoethylene glycols, cyclic conjugated annulenes, and cyclic non-conjugated crown ethers. Chemical structures or formulas also provided.

5   Scaling of Lattice Parameters

In order to isolate the impact of molecular packing from molecule density in determining dielectric properties of a lattice, lattice parameters in SC and BCC lattices of C_{60} are scaled in order to produce the same molecule density as experimentally reported FCC lattices. Similarly, lattice parameters in experimentally reported PCBM lattices as deposited from CB and oDCB are scaled to reproduce the molecule density of experimentally reported SF lattices.

In both cases, this is achieved by scaling each lattice vector by a quantity k, given by:

$$k = \left(\frac{N' V'_u s'_a s'_b s'_c}{N V_u s_a s_b s_c} \right) \tag{6}$$

Where N represents the number of fullerene molecules in the unit cell, V_u represents the volume of the unit cell, and s_a, s_b, and s_c represent the number of unit cells in the lattice in directions $\vec{a}$, $\vec{b}$, and $\vec{c}$, respectively, of the lattice being scaled to (ie. FCC C_{60} and SF PCBM lattices). N', V'_u, s'_a, s'_b, and s'_c represent similar quantities in the original structure of the lattice being scaled (ie. SC or BCC C_{60}, and CB or oDCB PCBM). The resulting lattice parameters presented in Tables 1 and 2.

6

Table 1 Lattice Parameters in 10x10x10 FCC C_{60} lattice, and density scaled versions of BCC and SC lattices.

	FCC	BCC	SC
Lattice Size	10x10x10	8x16x16	12x18x18
N	4631	4649	4693
Side length (a_0)	26.555	20.938	16.96

Table 2 Lattice Parameters in solvent-free PCBM lattice, and as deposited from CB and o-DCB, both unscaled, and density scaled to the solvent-free lattice.

	Unscaled Side Lengths			Scaled Side Lengths		
	a/a_0	b/a_0	c/a_0	a/a_0	b/a_0	c/a_0
Solvent-free	25.502	28.643	36.087	25.502	28.643	36.087
CB	26.141	28.89	36.376	25.773	28.483	35.863
o-DCB	25.996	31.434	36.05	24.972	30.196	34.63

6   Lattice Size Dependence of Dielectric Properties of Fullerenes

Size dependence of dielectric properties of C_{60} and PCBM in a range of lattice structures are shown in Figures 5 and 6. Values for the largest lattices are given in the main text.
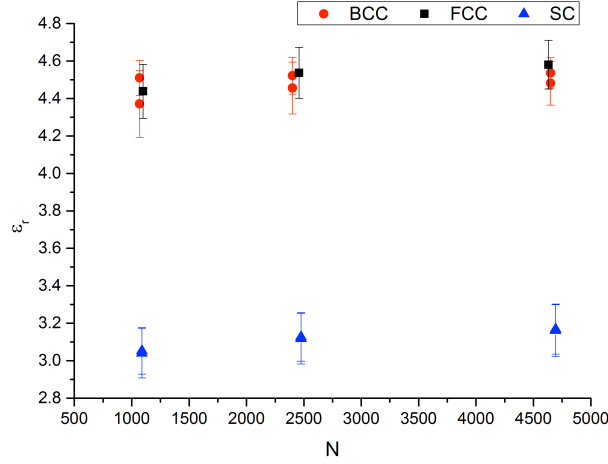
Figure 5 Lattice Size Dependence of Dielectric Properties of C$_{60}$ in Density Scaled FCC, BCC, and SC Lattice Structures Lattice size dependence of dielectric constant, $\epsilon_{r,x}$, calculated using Equation 5, against total number of molecules in FCC, BCC and SC lattices, with number densities of molecules scaled to that of the experimentally reported FCC lattice. Error bars in (b) indicate deviations from a $^1/_r$ relationship between binding energy and separation. BCC and SC lattice sizes were chosen such that they have a similar number of molecules to cubic lattices of FCC with side lengths of 6,8, and 10 lattice vectors. As a result BCC, and SC lattices have unequal numbers of lattice vectors in each direction ($6 \times 6 \times 12$, $6 \times 6 \times 12$, $8 \times 8 \times 16$, $8 \times 16 \times 16$ in BCC, $8 \times 10 \times 10$, $10 \times 14 \times 14$, $12 \times 18 \times 18$ in SC), and multiple points are included for a single size in these lattices, indicating charge separation along different lattice vectors.
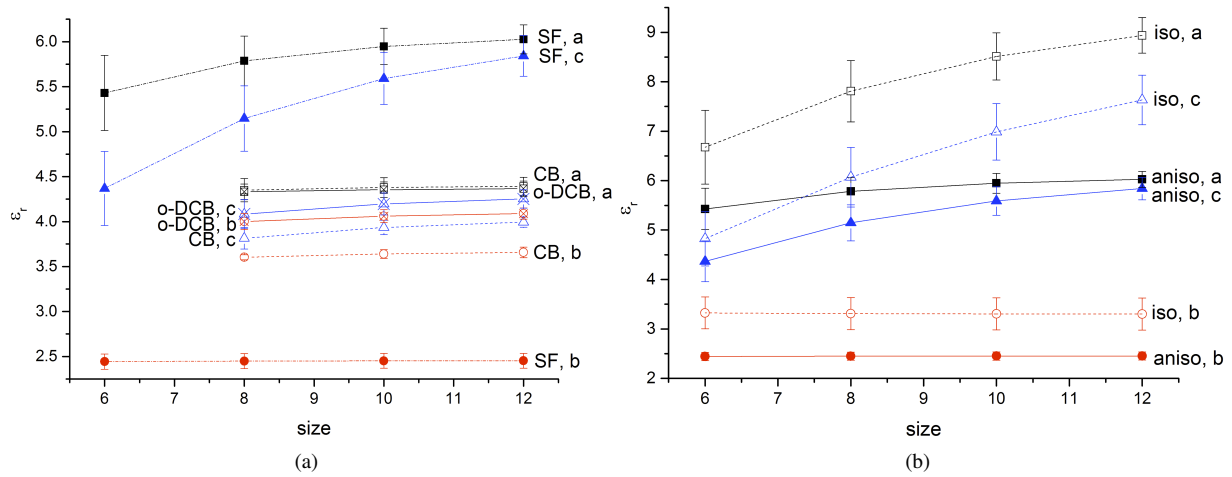

Figure 6 Lattice Size Dependence of Dielectric Properties of PCBM in a range of Lattice Structures (a) Diagonal components of the Dielectric tensor along lattice directions a, b, and c, as calculated using Equation 5, against cubic lattice size for SF, CB and o-DCB, with the number densities of CB and o-DCB lattices scaled to that of solvent-free lattices. (b) As (a) in SF lattice, but compared the same quantity calculated with the polarisability tensor of each PCBM molecule replaced with an isotropic tensor of the same α_{mean}. Error bars indicate deviations from a $^1/_r$ relationship between binding energy and separation.

8

7   Slices through PCBM Crystals as Deposited from Chlorobenzene and Ortho-Dichlorobenzene

Figure 7 shows slices through a solvent-free PCBM crystal structure, and PCBM as deposited from chlorobenzene and ortho-dichlorobenzene.
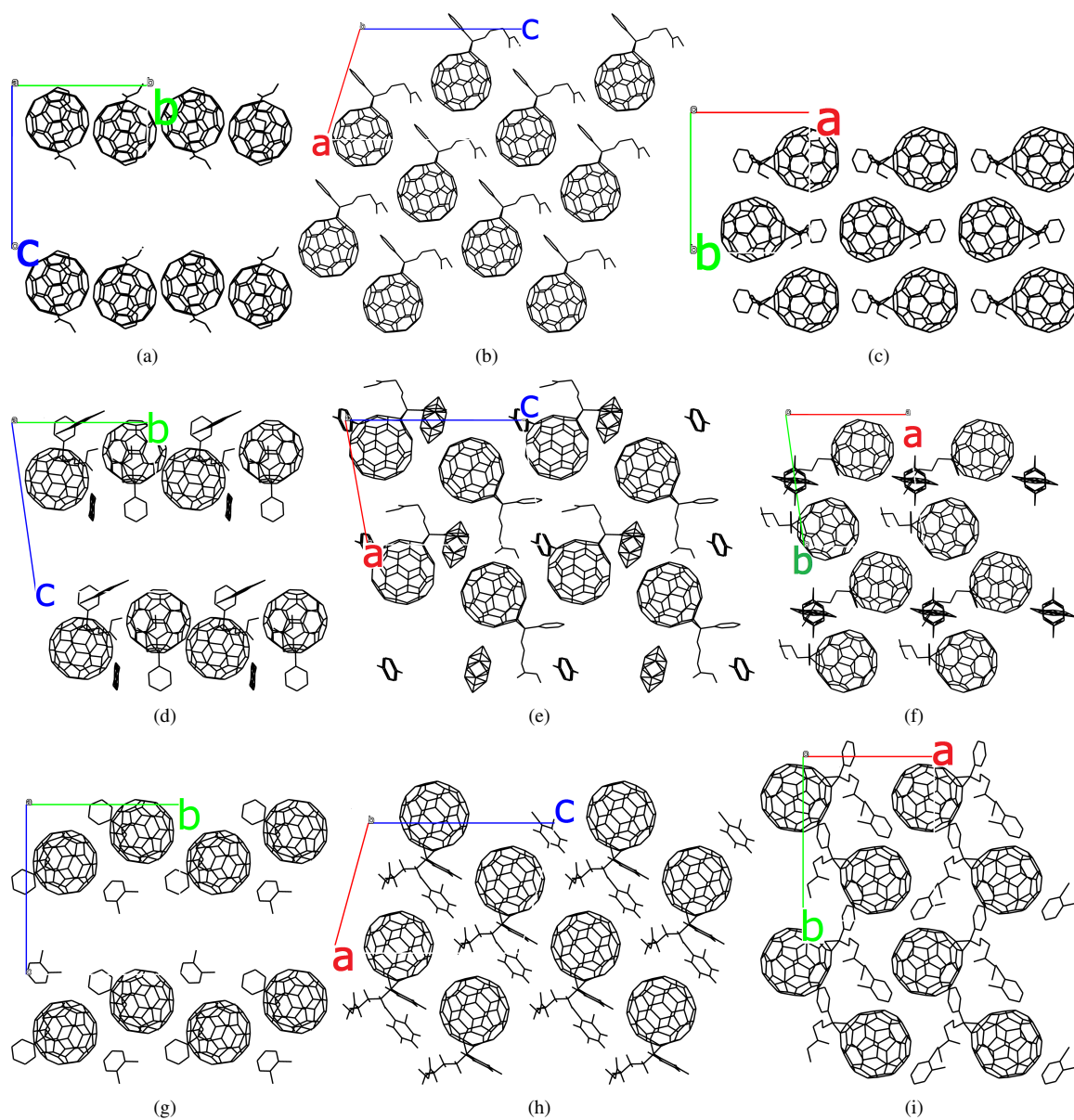
Figure 7 Slices through PCBM Crystals, (a-c) Solvent-Free and as Deposited from (d-f) Chlorobenzene and (g-i) Ortho-Dichlorobenzene (a,d,g) viewed along a, sliced between (a) 0.5a and 1.0a, and (d,g) 0.0a and 0.5a, (b,e,h) viewed along b, sliced between (a,e) 0.0b and 0.5b, and (b) 0.5b and 1.0b, (c,f,i) viewed along c, sliced between 0.0c and 0.5c.[5,6] Differences in slicing are such as to include molecule 1 (as defined in Figure 5 of the main text) in each case.

References

[1] H. A. Stern, G. A. Kaminski, J. L. Banks, R. Zhou, B. J. Berne and R. A. Friesner, *The Journal of Physical Chemistry B*, 1999, **103**, 4730–4737.

[2] B. Thole, *Chemical Physics*, 1981, **59**, 341–350.

[3] C. F. Macrae, I. J. Bruno, J. a. Chisholm, P. R. Edgington, P. McCabe, E. Pidcock, L. Rodriguez-Monge, R. Taylor, J. van de Streek and P. a. Wood, *Journal of Applied Crystallography*, 2008, **41**, 466–470.

[4] S. Belongie, *MathWorld–A Wolfram Web Resource.*

[5] M. Casalegno, S. Zanardi, F. Frigerio, R. Po, C. Carbonera, G. Marra, T. Nicolini, G. Raos and S. V. Meille, *Chemical Communications (Cambridge, England)*, 2013, **49**, 4525–7.

[6] M. T. Rispens, A. Meetsma, R. Rittberger, C. J. Brabec, N. S. Sariciftci and J. C. Hummelen, *Chemical Communications (Cambridge, England)*, 2003, **17**, 2116–8.